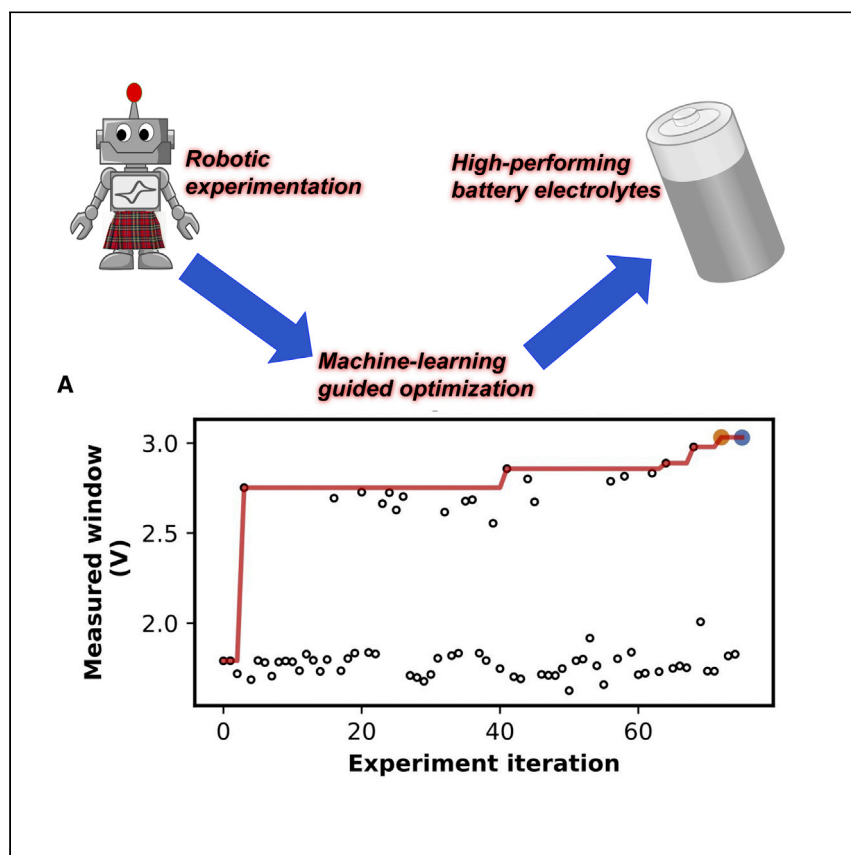


Article

# Autonomous Discovery of Battery Electrolytes with Robotic Experimentation and Machine Learning



Dave et al. combine robotics and machine learning to discover aqueous electrolytes. The algorithm runs the experiment without human intervention, delivering a mixed-anion sodium electrolyte with non-intuitively better performance compared to the benchmark. A dataset of 251 blended-salt aqueous electrolytes that includes conductivities, pHs, and electrochemistry electrolytes is obtained.

Adarsh Dave, Jared Mitchell, Kirthevasan Kandasamy, ..., Barnabás Póczos, Jay Whitacre, Venkatasubramanian Viswanathan

whitacre@andrew.cmu.edu (J.W.)  
venkvis@cmu.edu (V.V.)

## HIGHLIGHTS

Robotics and machine learning combine to autonomously find aqueous electrolytes

A non-intuitive, mixed-anion sodium electrolyte is discovered

251 mixed-salt electrolytes' conductivities, electrochemical behavior, and pHs are examined

Article

# Autonomous Discovery of Battery Electrolytes with Robotic Experimentation and Machine Learning

Adarsh Dave,<sup>1,4</sup> Jared Mitchell,<sup>2</sup> Kirthevasan Kandasamy,<sup>3,5</sup> Han Wang,<sup>2</sup> Sven Burke,<sup>2</sup> Biswajit Paria,<sup>3</sup> Barnabás Póczos,<sup>3</sup> Jay Whitacre,<sup>2,4,\*</sup> and Venkatasubramanian Viswanathan<sup>1,4,\*</sup>

## SUMMARY

Innovations in batteries can require years of experimentation for design and optimization. We report an autonomous approach to the optimization of a battery electrolyte that uses machine learning coupled to a robotic test-stand to perform hundreds of sequential experiments. We search for mixtures of salts in aqueous electrolytes with high electrochemical stability using Bayesian optimization. In 40 hours of experimentation testing for 140 electrolyte formulas, we converge on a non-intuitive optimal electrolyte. The optimum is a mixed-anion sodium electrolyte that is more stable than a benchmark electrolyte, despite lower salt content, contrary to the known design principle. The precision and repeatability of the robotic test-stand distinguishes formulations that human-guided design may have missed. Our result demonstrates the possibility of integrating robotics with machine learning to discover novel battery materials. We provide a dataset characterizing 251 aqueous electrolytes containing  $\text{LiNO}_3$ ,  $\text{LiClO}_4$ ,  $\text{Li}_2\text{SO}_4$ ,  $\text{NaNO}_3$ ,  $\text{NaClO}_4$ , and  $\text{Na}_2\text{SO}_4$  that includes conductivities, pHs, and electrochemical responses on platinum.

## INTRODUCTION

Energy-dense and safe batteries are crucial for the electrification of transportation<sup>1</sup> and aviation.<sup>2</sup> However, improvements to battery materials can take years to deliver and many iterations of testing might be required to optimize the material to achieve the objectives.<sup>3</sup> The battery-design problem is fundamentally a complex function that takes battery formulation as input and outputs performance measurements. Machine-learning methods can be used to optimize these black-box functions.<sup>4–8</sup> Machine-learning models coupled to automated evaluation — able to immediately act on the model's recommendations — can “close the loop” and enable inverse material design.<sup>9–14</sup> Bayesian optimization in particular has been proven effective in solving chemical design problems over minimal experimental iterations, with successful examples including carbon nanotube<sup>15</sup> and polymer fiber synthesis,<sup>16</sup> meta-material design,<sup>17</sup> and organic photovoltaic devices.<sup>18</sup> Although similar approaches have been attempted in several fields of study, to our knowledge this is the first attempt to apply this framework to the design of functional materials in electrochemistry.

We have built the robotic platform “Otto” from scratch for characterizing battery electrolytes,<sup>19,20</sup> and the schematic is shown in Figure 1. In this work, we connected our platform to a Bayesian optimizer and allowed it to run autonomously, allowing the machine-learning model to plan each experiment sequentially on the basis of

<sup>1</sup>Department of Mechanical Engineering, Carnegie Mellon University, Pittsburgh, PA 15213, USA

<sup>2</sup>Department of Materials Science and Engineering, Carnegie Mellon University, Pittsburgh, PA 15213, USA

<sup>3</sup>Department of Machine Learning, Carnegie Mellon University, Pittsburgh, PA 15213, USA

<sup>4</sup>Wilton E. Scott Institute for Energy Innovation, Carnegie Mellon University, Pittsburgh, PA 15213, USA

<sup>5</sup>Present address: Department of Electrical Engineering and Computer Sciences, University of California, Berkeley, Berkeley, CA 94709, USA

\*Correspondence: [whitacre@andrew.cmu.edu](mailto:whitacre@andrew.cmu.edu) (J.W.), [venkvis@cmu.edu](mailto:venkvis@cmu.edu) (V.V.)

<https://doi.org/10.1016/j.xcrp.2020.100264>

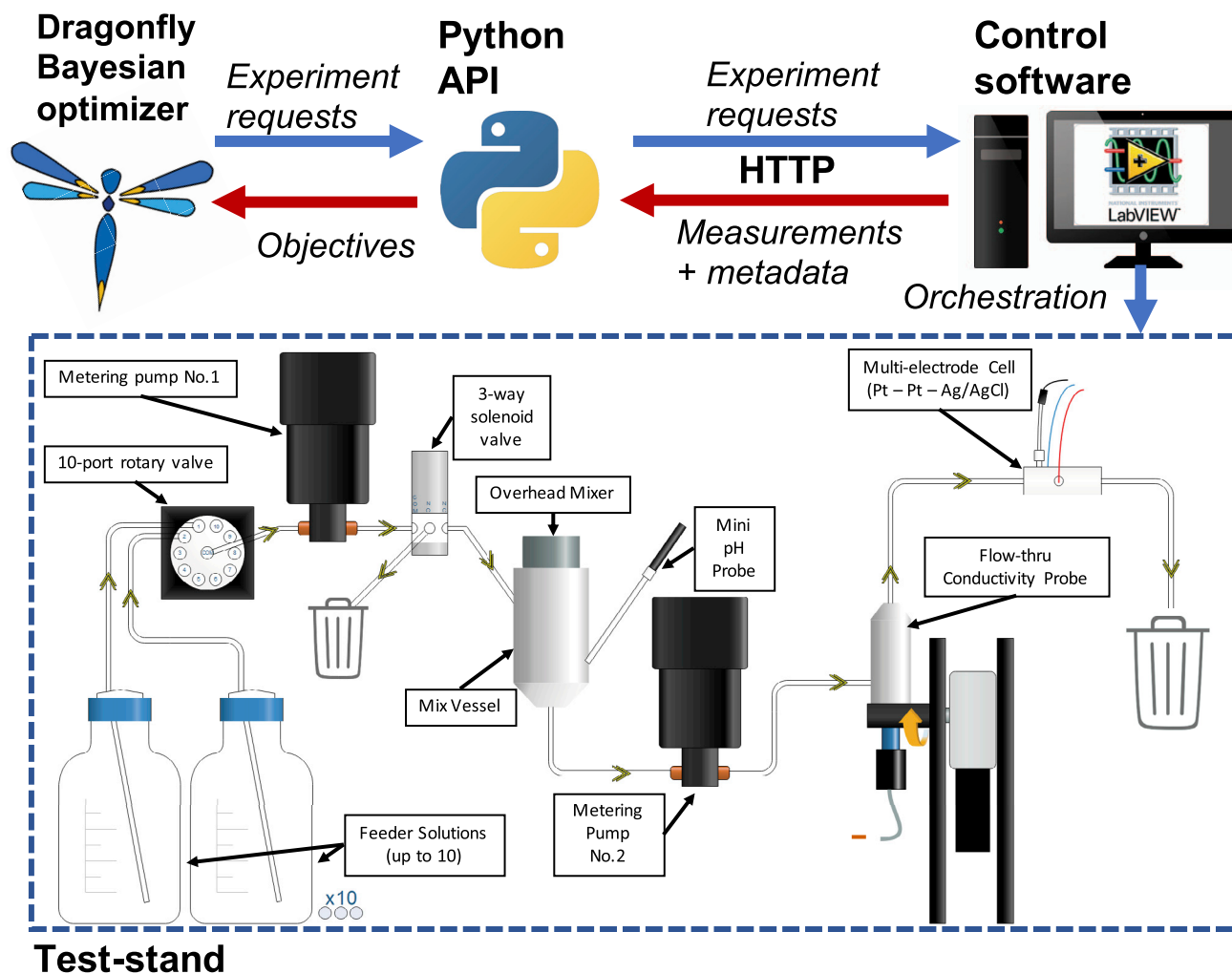


**Figure 1. Schematic Figure of Robotic Platform and Software Architecture**

The test-stand (Otto) mixes feeder solutions and measures pH, ionic conductivity, and electrochemical properties in a symmetric platinum electrode cell. The control software takes in an experiment request and returns measurements and metadata (e.g., temperature) over HTTP to a Python API. Dragonfly, the Bayesian optimization software utilized, plugs into the Python API for requesting experiments and receiving feedback. A more detailed version of test-stand components and logic is available as [Figure S8](#).

measurement feedback in real time. Our goals are: (1) to demonstrate and assess the first attempt of battery electrolyte design by machine-learning integrated into robotics, (2) to confidently optimize in previously unexplored design spaces, (3) to discover interesting, non-intuitive, and high-performing materials with this method, and (4) to generate high-quality data for the community and make it available with all metadata in a structured format.

We specifically target aqueous electrolyte design with our method and look to maximize the electrolyte's electrochemical stability window in two design spaces: one space mixing three common lithium salts in water, and the other mixing four sodium salts in water. Three- or four-salt aqueous electrolytes have not yet appeared in the literature. Run continuously over a two-week period, Otto generated about 70 data points in each design space, which, with many additional experiments for replication and detailed evaluation, yielded over 250 experimental data points for a range of mixed-salt aqueous electrolytes. These data (electrolyte composition versus

conductivity, pH, and electrochemical assessment on platinum) are supplied in a easily queried format for the community (<https://data.matr.io/5>).

Aqueous electrolytes are of great research interest because the non-aqueous electrolytes commonly used in batteries are flammable and present significant safety hazards and manufacturing costs relating to safety, storage, and management.<sup>21,22</sup> Aqueous electrolytes are an attractive alternative. They are safer, lower-cost, and more conductive than non-aqueous counterparts.<sup>23,24</sup> High conductivity particularly suits large-format batteries that might be used in the electrical grid to smooth out the intermittent generation of power from renewable sources.<sup>25</sup>

However, aqueous electrolytes have a narrow electrochemical stability window, limited by the hydrogen evolution reaction (HER) at low electrochemical potentials and the oxygen evolution reaction (OER) at high potentials.<sup>26</sup> These parasitic reactions preclude the use of the high-voltage electrode couples that enable the high energy density of non-aqueous batteries<sup>21</sup> and lead to poor cycling capability, calendar life, and diminished high-rate performance.<sup>27</sup> A recent trend in aqueous electrolyte design uses very high salt concentrations to suppress these reactions, either by the deposition of a passivating electrode film (often via anionic reduction) or by modifying interfacial hydration structures to achieve similar effects. These “water-in-salt” electrolytes have been shown to expand the electrochemical stability window from less than 2V for a standard aqueous electrolyte up to 3V, with effects demonstrated in both lithium and sodium systems.<sup>22,28–31</sup> Water concentration alone has been shown to have asymmetric influence on electrolyte resistance to HER and OER.<sup>29</sup> Blending salts in electrolytes can positively impact performance, opening the possibility for mixed-anion electrolytes with improved electrochemical windows,<sup>32,33</sup> but three- and four-salt aqueous electrolytes have not appeared in the literature.

Improvements in stability for aqueous electrolytes that do not reduce into a passivating film are not fully explained from first principles.<sup>28,29,34,35</sup> Because these systems have properties that are expensive to compute with molecular dynamics, the computational screening of aqueous electrolytes would be challenging and time-consuming without guarantee of fidelity when compared to physical experimentation. Progress in aqueous electrolyte design is made via chemists’ ingenuity and a significant amount of manual testing.

We reformulate aqueous electrolyte design as a black-box optimization problem. Otto mixes together aqueous electrolyte salts, pre-dissolved near saturation into feeder solutions, and measures two electrolyte objectives: ionic conductivity and electrochemical stability, as well as temperature and pH. Electrochemical stability is tested with constant current holds at four current levels (111, 22, 5, then 1 mA/cm<sup>2</sup>, first testing OER onset potentials then HER onset potentials) on two platinum wires with an Ag/AgCl reference electrode. As described previously,<sup>19</sup> we utilize a slope-extrapolation method between 22 and 5 mA/cm<sup>2</sup> to the zero-current axis to characterize electrolyte stability. This method will over-estimate electrolyte stability compared to longer measurements done at a lower currents (e.g., 50 μA/cm<sup>2</sup>), but using this quantity during survey and optimization enables a 60 s measurement of electrolyte stability against HER and OER with consistent variance.<sup>19</sup> Dosing, mixing, measurement, flushing, and washing steps meant that each experimental iteration took under 25 min. In-depth details on the design, calibration, and performance of Otto and the fast electrochemical assessment are previously published,<sup>19</sup> but a detailed schematic of the test-stand mechanics and visualizations of the test are shown in [Figures S1–S4](#) and [S8](#).

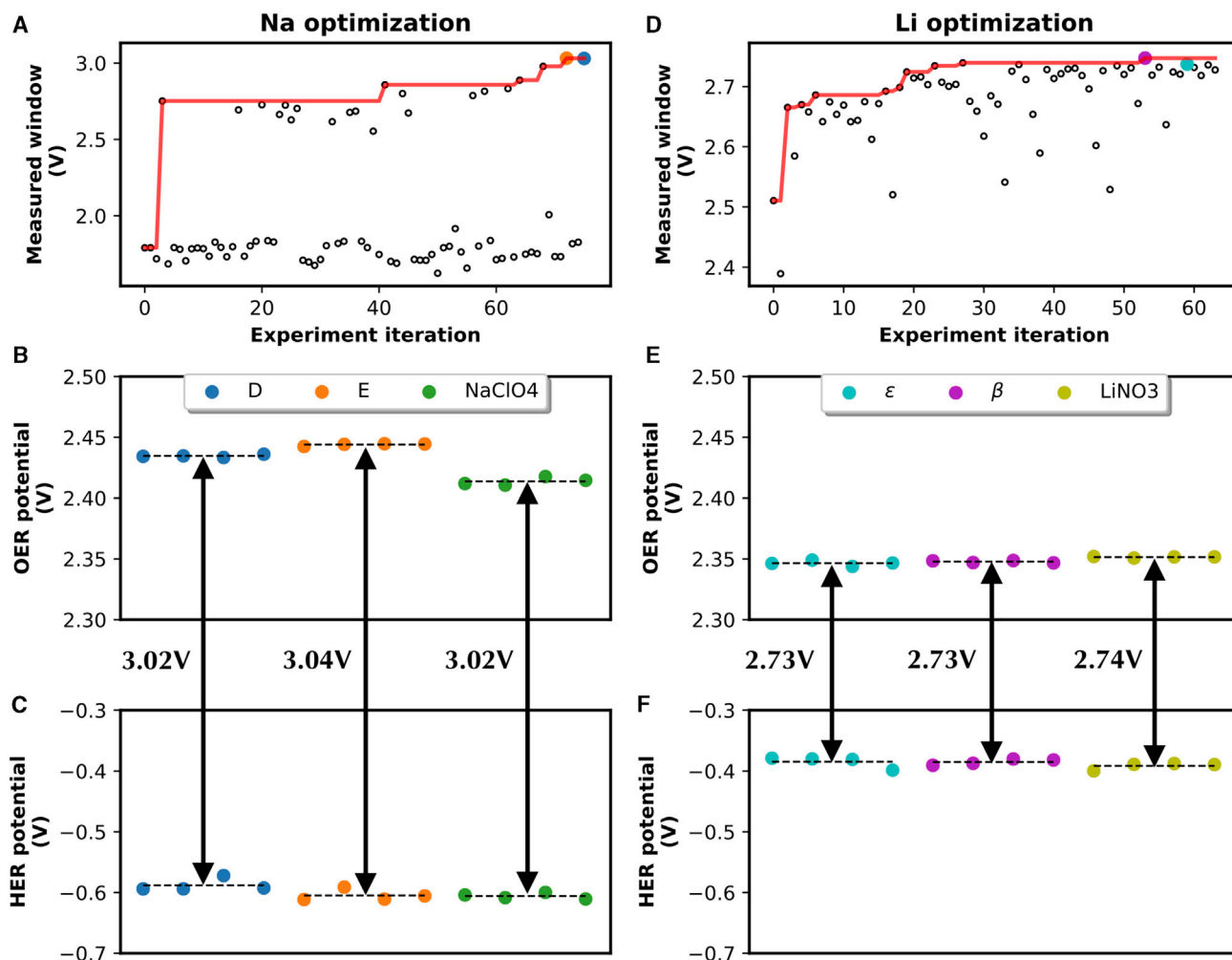


**Figure 2. Results for Autonomous Optimization of Aqueous Electrolytes**

Sodium (left column) and lithium (right column) design spaces comprise the two columns.

(A and D) The panels show Dragonfly's optimization routine for sodium (A) and lithium (D). The black circles indicate individual evaluations, and the red line shows the maximum stability window found over iterations. Shown in color are the top blends found by Dragonfly, the compositions of which are given in Table 1.

(B, C, E, and F) For each top blend, four additional experiments were carried out against baselines of NaClO<sub>4</sub> and LiNO<sub>3</sub>, and the potentials (via slope-extrapolation method) are reported here. The OER (B) and HER (C) potentials of Blends D and E were compared to NaClO<sub>4</sub>. The OER (E) and HER (F) potentials of Blends ε and β were compared to LiNO<sub>3</sub>. Blend E is the best-performing sodium electrolyte, and LiNO<sub>3</sub> is the best lithium electrolyte.

The optimal electrolyte found in the sodium design space is a novel dual-anion sodium electrolyte. The blended electrolyte exhibits a wider electrochemical stability window on platinum compared to a baseline NaClO<sub>4</sub> aqueous sodium electrolyte,<sup>30,35</sup> despite lower overall salt content. The electrolyte can be used in a cell with repeated cycling at over 2V reversible capacity on active electrodes. The automated discovery of a non-intuitive, novel electrolyte in a complex design space illustrates the promise of using machine learning coupled to robotic experiments to rapidly optimize material designs that human experimenters might miss.

## RESULTS AND DISCUSSION

### Manual Surveys

Otto first surveyed electrochemical stability as a function of salt concentration on a manually defined grid across common lithium and sodium electrolytes without the

**Table 1. Concentrations of Feeder Solutions**

Feeder Solution	Molality
NaClO <sub>4</sub>	16.03
NaNO <sub>3</sub>	10.03
Na <sub>2</sub> SO <sub>4</sub>	1.5
NaBr	8
LiNO <sub>3</sub>	7.02
Li <sub>2</sub> SO <sub>4</sub>	3.01
LiClO <sub>4</sub>	5.01

Feeder solutions were made near each salt's solubility limit in water by molality and mixed to create each electrolyte formulation.

machine-learning optimizer. The results, shown in [Figure S9](#), demonstrate significant differences in behavior among salts in suppressing OER and HER when controlling for salt content. These results motivated our design problem where salts are chosen and blended to discover a novel electrolyte with an optimal stability window.

### Machine-Learning-Guided Optimization

It would be time consuming to exhaustively search mixtures of these anions for optimal formulations because the complexity of these design spaces exhibits combinatorial explosion. For example, Otto utilizes a testing volume of 7 mL. Exhaustively searching a space of 3-salt mixtures in 0.1 mL increments would require 62,000 evaluations, and a space of 4-salt mixtures would require 1,150,000 evaluations. To make optimization over this design space practical, we connected Otto to Dragonfly, a Bayesian optimization software package developed by our team. Dragonfly harnesses a suite of acquisition strategies and evolutionary algorithms for scalable and robust treatment of black-box functions.<sup>6,7</sup> Although other Bayesian optimization packages (e.g., GPyOpt, BOTorch) are widely used, Dragonfly is unique in its adaptive sampling strategy. Other packages enforce a choice of a single acquisition function, which can lead to problem-dependent performance. Dragonfly uses four different acquisition functions and actively learns which performs best in the task at hand through the course of each optimization run.<sup>7</sup> The combined approach can be important for problems in which the optimization response surface is unknown. Also, interfacing directly to an experiment requires support for optimizing under arbitrary constraints and discrete domains, which was developed in Dragonfly for this work.

Given only solubility and pumping-precision constraints on mixtures, Dragonfly optimized for the electrochemical stability window — as measured by the fast electrochemical assessment and summarized into a single value with a slope-extrapolation method — over the design spaces of (1) mixtures of NaNO<sub>3</sub>, NaClO<sub>4</sub>, Na<sub>2</sub>SO<sub>4</sub>, and NaBr and (2) mixtures of LiNO<sub>3</sub>, LiClO<sub>4</sub>, and Li<sub>2</sub>SO<sub>4</sub>. Dragonfly operated fully autonomously, running experiments with no human guidance. Results are illustrated in [Figures 2A–2F](#). Concentrations of feeder solutions for each salt are given in [Table 1](#); compositions of the blended electrolytes discovered by Dragonfly that have the widest measured stability windows are given in [Table 2](#).

The optimization curve over sodium electrolytes illustrated in [Figure 2A](#) looks split. Any amount of NaBr in the electrolyte significantly lowered cathode stability due to an anodic reaction of the bromide anion; in other words, a non-smooth chemical response appeared along the NaBr axis. This quality of the design space is apparent when the stability window is viewed against the electrolyte components' Euclidean distance ([Figure S13](#)) and compared to that of the lithium design space ([Figure S14](#)).

**Table 2. Composition of Electrolyte Blends Discovered**

Blend	Composition (mL of feeder solutions)
D	6.1 NaClO <sub>4</sub> , 0.8 NaNO <sub>3</sub> , 0.1 Na <sub>2</sub> SO <sub>4</sub>
E	6.7 NaClO <sub>4</sub> , 0.3 NaNO <sub>3</sub>
E	6.4 LiNO <sub>3</sub> , 0.6 LiClO <sub>4</sub>
B	5.7 LiNO <sub>3</sub> , 0.9 LiClO <sub>4</sub> , 0.4 Li <sub>2</sub> SO <sub>4</sub>

Test volume was kept constant at 7mL.

Gaussian process regression requires an assumption of smoothness on the response surface.<sup>7</sup> The underlying Gaussian process regression model used in the sodium design space was probably not very well-fitted to sampled data during the first half of optimization. In [Figure 3](#), we re-run this optimization on the sodium design space after log-scaling the NaBr axis. Log-scaling gives the response surface smaller gradients along this axis, and encoding this information *a priori* enables much improved performance: “bo-log” shows faster convergence to the optimum and more consistent adaptive sampling compared to “bo.” As always, selection and presentation of the design space is of utmost importance to autonomous design tasks.

Top blends from the sodium optimization in [Figure 2](#) were run for an additional four experiments each against a pure NaClO<sub>4</sub> feeder-solution benchmark. The four measured potentials and their averages are reported in [Figures 2B](#) and [2C](#). Blend E showed an improved OER stability of 20 mV over pure NaClO<sub>4</sub>.

The optimization over lithium electrolytes is illustrated in [Figure 2D](#). Dragonfly initializes by randomly sampling the design space in the first five runs, which, in the case of the lithium design space, included a strong electrolyte. The three-dimensional design space is smaller than the sodium design space and exhibits a smooth response to electrolyte formulation ([Figure S14](#)). Our optimization converges faster than the other design space. The optimizer converged on two blends and pure LiNO<sub>3</sub> feeder solution as three candidates with optimal stability windows; other high-performing candidates were dilutions of LiNO<sub>3</sub> and not tested. These electrolytes were run for an additional four experiments each; the measured potentials are shown in [Figures 2E](#) and [2F](#). The concentrated LiNO<sub>3</sub> electrolyte is the strongest performer tested by the optimizer. Its use has been reported in literature.<sup>26,28</sup>

### Detailed Evaluation of Optimal Electrolytes

Blend E and NaClO<sub>4</sub> were run for a longer, detailed evaluation of OER stability in Otto, illustrated in [Figure 4](#). Current density was varied in half log-decade steps from  $j = 10^{-1} \text{ A/cm}^2$  to  $10^{-5} \text{ A/cm}^2$ . A Tafel equation was fit to the average of seven sequential runs, ignoring high current steps  $j = 10^{-1}$  and  $10^{-1.5} \text{ A/cm}^2$ . Otto has previously been used to replicate the Tafel slope of 1M KOH standard for OER posited in the literature<sup>36</sup> to within experimental error ([Figure S5](#)). Full data figures and methods for this run are given in the [Supplemental Experimental Procedures](#) and [Figures S6](#) and [S7](#). The results show that Blend E is more resistant to OER on platinum than high-concentration NaClO<sub>4</sub>, a high-performing sodium electrolyte extensively evaluated in past work.<sup>30,31,35</sup> The potential at a low leakage current<sup>34</sup> ( $30 \mu\text{A/cm}^2$ ) is 24 mV higher in the blend than in the NaClO<sub>4</sub> feeder solution. The blend also shows significantly higher resistance to OER at high potentials with a 58% suppression of current density at 2V compared to the NaClO<sub>4</sub> feeder solution.

Although a 24 mV improvement does not constitute a state-of-the-art aqueous battery electrolyte, this result is interesting for a number of reasons. First, Blend E has a

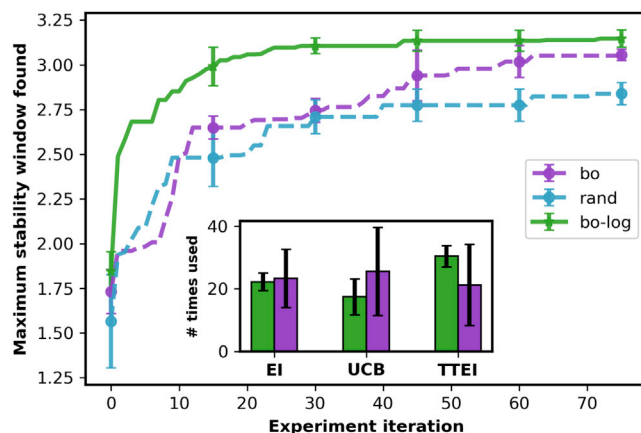


**Figure 3. Assessing Optimization along a Non-smooth Response**

The sodium optimization was re-run synthetically (see “Synthetic Optimization” in the [Supplemental Experimental Procedures](#)) to examine the non-smooth response along the NaBr axis. Each series reflects the mean  $\pm$  standard deviation of five optimization runs. When comparing random sampling (“rand”), to vanilla Bayesian optimization in Dragonfly (“bo”), to the same with a log-scaled NaBr axis (“bo-log”), “bo-log” improves convergence to the optimum in the design space; adaptive sampling is more consistent in choice of acquisition function, reflecting more stable optimizations due to a better-fitting underlying model.

higher water concentration compared to the  $\text{NaClO}_4$  solution but exhibits increased stability against OER, which is contrary to the generally followed design principle. Further evaluations of small additions of  $\text{NaNO}_3$  to high-concentration  $\text{NaClO}_4$  near the ratio of Blend E show that even less added  $\text{NaNO}_3$  can have a similar effect of improving OER stability, despite lower overall salt concentration ([Figures S10 and S11](#)). The mixed-anion character of Blend E might more significantly suppress water activity at interfaces,<sup>28</sup> with minimal changes to the bulk properties of the  $\text{NaClO}_4$  solution (i.e.,  $\text{NaNO}_3$  appears to function like an additive improving OER stability). A full cell was constructed using  $\text{NaTi}_2(\text{PO}_4)_3$  and activated carbon as the anode and cathode (here, as an electrochemical double-layer capacitor), respectively, with Blend E as the electrolyte. The cell can operate at well over 2V over many cycles as shown in [Figure S12](#). Second, the discovered electrolyte is only four parts in 100 different from the benchmark, on the scale of an additive (e.g., five parts in 100 vinylene carbonate in nonaqueous chemistries<sup>37</sup>). A small effect due to a small change in the electrolyte is discovered with machine learning and automation assistance. We reproduce this result on command, as illustrated in the dataset provided and in [Figures 2B and 3](#) and [Figures S6, S7, S10, and S11](#).

We note that this method and the required equipment was inexpensive and consisted solely of high-precision pumping units, custom-machined PTFE fixtures, and standard electrochemical tooling in the Consort probe and a Palmsens 4. The test-stand was operated by two team members. In our example, automation and machine learning acted as a “force multiplier” for a small team.

In this work, we have demonstrated the first automated design of battery electrolytes by machine learning integrated into robotics. We have optimized two previously unexplored design spaces and find an interesting and non-intuitive optimum, while generating a database on aqueous electrolytes. All data captured by Otto are made available in a structured format that gives the full concentration dependence of ionic conductivity, pH, and electrochemical behavior via multi-step potentiometry



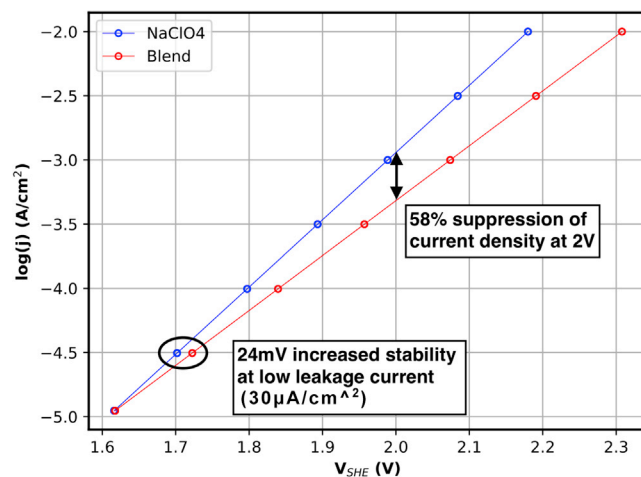


**Figure 4. Re-evaluating the Optimal Electrolyte outside Otto**

Results for seven runs on Blend E against the control NaClO<sub>4</sub> suggest that the blend is better at suppressing OER than NaClO<sub>4</sub>. The potential for an acceptable leakage current (30  $\mu\text{A}/\text{cm}^2$ ) is 24 mV higher in the blend, and the blend illustrates significantly improved high-rate capability with a 58% (–0.37 log units) suppression of current density at 2V compared to NaClO<sub>4</sub>. The two electrolytes are close in pH (near 8.8); the potentials given are therefore not pH shifted.

on platinum for all salts mentioned. Exhaustive data for the single salts, as well as 167 samples requested during machine-learning-guided stability-window optimization, are present in the dataset. We believe these data are useful not just to the battery community but also to those in adjacent fields (e.g., catalysis in aqueous environments). This result demonstrates an important proof-point of the ability of autonomous platforms to accelerate material optimization.

## EXPERIMENTAL PROCEDURES

### Resource Availability

#### Lead Contact

J. Whitacre and V. Viswanathan are reachable at [whitacre@andrew.cmu.edu](mailto:whitacre@andrew.cmu.edu) and [venkvis@cmu.edu](mailto:venkvis@cmu.edu) respectively.

#### Materials Availability

This study did not generate new unique reagents.

#### Data and Code Availability

The public dataset is available at <https://data.matr.io/5> and contains all electrolyte formulations tested relevant to this work. It contains conductivity, pH, and multi-step potentiometry measurements of 251 different electrolyte formulations of common lithium and sodium salts. Exhaustive data give the concentration dependence of measured properties in the cases of LiNO<sub>3</sub>, LiClO<sub>4</sub>, Li<sub>2</sub>SO<sub>4</sub>, NaNO<sub>3</sub>, NaClO<sub>4</sub>, Na<sub>2</sub>SO<sub>4</sub>, and NaBr, as well as a machine-learning-guided sampling of mixtures of these salts. These data support [Figures 2](#) and [S9](#).

The supporting data for the other included graphs within this paper, as well as other findings from this study, are available from the corresponding author upon reasonable request.

Dragonfly is open source and publicly available at <https://github.com/dragonfly/dragonfly/>

The code for the plots presented in this paper is available from the corresponding author upon reasonable request.

### SUPPLEMENTAL INFORMATION

Supplemental Information can be found online at <https://doi.org/10.1016/j.xcrp.2020.100264>.

### ACKNOWLEDGMENTS

This work was supported by the Toyota Research Institute through the Accelerated Materials Design and Discovery program. The authors acknowledge insightful discussions with Brian Storey, Abraham Anapolsky, Linda Hung, and Chirranjeevi Gopal from the Toyota Research Institute and Wei Wu from Carnegie Mellon University.

### AUTHOR CONTRIBUTIONS

J.W., V.V. and B. Póczos conceived the project. J.M. designed, machined, and assembled the test-stand and wrote Labview control software. J.M. designed the fast electrochemical assessment. A.D. designed Python software and the data layer and web-server interface. S.B. prepared all feeder solutions and stocked the test-stand. A.D. managed experiments (data input and output for the test-stand both in manually defined and machine-learning-operated modes) and analyzed results. K.K. and B. Paria wrote Dragonfly, consulted on its applicability to this problem and its results, and implemented required features for running Otto from Dragonfly. A.D. and V.V. wrote the paper with input from all the authors. A.D. and J.M. produced all the figures.

### DECLARATION OF INTERESTS

The authors declare no competing interests.

Received: October 12, 2020

Revised: October 27, 2020

Accepted: October 30, 2020

Published: November 9, 2020

### REFERENCES

- Deng, J., Bae, C., Mariucci, J., Masias, A., and Miller, T. (2018). Safety modelling and testing of lithium-ion batteries in electrified vehicles. *Nat. Energy* 3, 261–266.
- Viswanathan, V., and Knapp, B.M. (2019). Potential for electric aircraft. *Nat. Sustain.* 2, 88–89.
- Tabor, D.P., Roch, L.M., Saikin, S.K., Kreisbeck, C., Sheberla, D., Montoya, J.H., Dwaraknath, S., Aykol, M., Ortiz, C., Tribukait, H., et al. (2018). Accelerating the discovery of materials for clean energy in the era of smart automation. *Nat. Rev. Mater.* 3, 5–20.
- Kandasamy, K., Schneider, J., and Póczos, B. (2015). High dimensional bayesian optimisation and bandits via additive models. In editors, Proceedings of the 32nd International Conference on Machine Learning, volume 37 of Proceedings of Machine Learning Research, F. Bach and D. Blei, eds. (Lille, France: PMLR), pp. 295–304.
- Kandasamy, K., Neiswanger, W., Zhang, R., Krishnamurthy, A., Schneider, J., and Póczos, B. (2019a). Myopic posterior sampling for adaptive goal oriented design of experiments. In editors, Proceedings of the 36th International Conference on Machine Learning, volume 97 of Proceedings of Machine Learning Research, K. Chaudhuri and R. Salakhutdinov, eds. (Long Beach, California, USA: PMLR), pp. 3222–3232.
- Paria, B., Kandasamy, K., and Póczos, B. (2019). A flexible framework for multi-objective bayesian optimization using random scalarizations. In Proceedings of the Thirty-Fifth Conference on Uncertainty in Artificial Intelligence, UAI 2019, Tel Aviv, Israel, July 22–25, 2019, p. 267.
- Kandasamy, K., Vysyaraju, K.R., Neiswanger, W., Paria, B., Collins, C.R., Schneider, J., Póczos, B., and Xing, E.P. (2019b). Tuning Hyperparameters without Grad Students: Scalable and Robust Bayesian Optimisation with Dragonfly. arXiv, 1903.06694.
- Hernández-Lobato, D., Hernández-Lobato, J.M., Shah, A., and Adams, R.P. (2016). Predictive entropy search for multi-objective bayesian optimization. *ICML*, 1492–1501.
- Kusne, A.G., Gao, T., Mehta, A., Ke, L., Nguyen, M.C., Ho, K.-M., Antropov, V., Wang, C.-Z., Kramer, M.J., Long, C., and Takeuchi, I. (2014). On-the-fly machine-learning for high-throughput experiments: search for rare-earth-free permanent magnets. *Sci. Rep.* 4, 6367.
- Zunger, A. (2018). Inverse design in search of materials with target functionalities. *Nat. Rev. Chem.* 2, 1–16.
- Granda, J.M., Donina, L., Dragone, V., Long, D.-L., and Cronin, L. (2018). Controlling an organic synthesis robot with machine learning to search for new reactivity. *Nature* 559, 377–381.
- Bhowmik, A., Castelli, I.E., Garcia-Lastra, J.M., Jørgensen, P.B., Winther, O., and Vegge, T. (2019). A perspective on inverse design of battery interphases using multi-scale modelling, experiments and generative deep learning. *Energy Storage Mater.* 21, 446–456.

13. Bai, Y., Wilbraham, L., Slater, B.J., Zwijnenburg, M.A., Sprick, R.S., and Cooper, A.I. (2019). Accelerated Discovery of Organic Polymer Photocatalysts for Hydrogen Evolution from Water through the Integration of Experiment and Theory. *J. Am. Chem. Soc.* *141*, 9063–9071.
14. Sun, S., Hartono, N.T.P., Ren, Z.D., Oviedo, F., Buscemi, A.M., Layurova, M., Chen, D.X., Ogunfunmi, T., Thapa, J., Ramasamy, S., et al. (2019). Accelerated Development of Perovskite-Inspired Materials via High-Throughput Synthesis and Machine-Learning Diagnosis. *Joule* *3*, 1437–1451.
15. Nikolaev, P., Hooper, D., Perea-López, N., Terrones, M., and Maruyama, B. (2014). Discovery of wall-selective carbon nanotube growth conditions via automated experimentation. *ACS Nano* *8*, 10214–10222.
16. Li, C., Rubin de Celis Leal, D., Rana, S., Gupta, S., Sutti, A., Greenhill, S., Slezak, T., Height, M., and Venkatesh, S. (2017). Rapid Bayesian optimisation for synthesis of short polymer fiber materials. *Sci. Rep.* *7*, 5683.
17. Bessa, M.A., Glowacki, P., and Houlder, M. (2019). Bayesian machine learning in metamaterial design: Fragile becomes supercompressible. *Adv. Mater.* *31*, e1904845.
18. MacLeod, B.P., Parlane, F.G.L., Morrissey, T.D., Häse, F., Roch, L.M., Dettelbach, K.E., Moreira, R., Yunker, L.P.E., Rooney, M.B., Deeth, J.R., Lai, V., Ng, G.J., Situ, H., Zhang, R.H., Elliott, M.S., Haley, T.H., Dvorak, D.J., Aspuru-Guzik, A., Hein, J.E., and Berlinguette, C.P. (2020). Self-driving laboratory for accelerated discovery of thin-film materials. *Sci. Adv.* *6*, eaaz8867.
19. Whitacre, J.F., Mitchell, J., Dave, A., Wu, W., Burke, S., and Viswanathan, V. (2019). An Autonomous Electrochemical Test Stand for Machine Learning Informed Electrolyte Optimization. *J. Electrochem. Soc.* *166*, A4181.
20. Dave, A., Gering, K.L., Mitchell, J.M., Whitacre, J., and Viswanathan, V. (2020). Benchmarking Conductivity Predictions of the Advanced Electrolyte Model (AEM) for Aqueous Systems. *J. Electrochem. Soc.* *167*, 013514.
21. Luo, J.-Y., Cui, W.-J., He, P., and Xia, Y.-Y. (2010). Raising the cycling stability of aqueous lithium-ion batteries by eliminating oxygen in the electrolyte. *Nat. Chem.* *2*, 760–765.
22. Suo, L., Borodin, O., Gao, T., Olguin, M., Ho, J., Fan, X., Luo, C., Wang, C., and Xu, K. (2015). “Water-in-salt” electrolyte enables high-voltage aqueous lithium-ion chemistries. *Science* *350*, 938–943.
23. Li, Z., Young, D., Xiang, K., Carter, W.C., and Chiang, Y.-M. (2013). Towards High Power High Energy Aqueous Sodium-Ion Batteries: The NaTi<sub>2</sub>(PO<sub>4</sub>)<sub>3</sub>/Na<sub>0.44</sub>mno<sub>2</sub> System. *Adv. Energy Mater.* *3*, 290–294.
24. Whitacre, J.F., Shanbhag, S., Mohamed, A., Polonsky, A., Carlisle, K., Gulakowski, J., Wu, W., Smith, C., Cooney, L., Blackwood, D., et al. (2015). A Polyionic, Large-Format Energy Storage Device Using an Aqueous Electrolyte and Thick-Format Composite NaTi<sub>2</sub>(PO<sub>4</sub>)<sub>3</sub>/Activated Carbon Negative Electrodes. *Energy Technol. (Weinheim)* *3*, 20–31.
25. Wu, W., Shabag, S., Chang, J., Rutt, A., and Whitacre, J.F. (2015). Relating Electrolyte Concentration to Performance and Stability for NaTi<sub>2</sub>(PO<sub>4</sub>)<sub>3</sub>/Na<sub>0.44</sub>mno<sub>2</sub> Aqueous Sodium-Ion Batteries. *J. Electrochem. Soc.* *162*, A803–A808.
26. Li, W., Dahn, J.R., and Wainwright, D.S. (1994). Rechargeable lithium batteries with aqueous electrolytes. *Science* *264*, 1115–1118.
27. Luo, J.-Y., and Xia, Y.-Y. (2007). Aqueous Lithium-ion Battery LiTi<sub>2</sub>(PO<sub>4</sub>)<sub>3</sub>/LiMn<sub>2</sub>O<sub>4</sub> with High Power and Energy Densities as well as Superior Cycling Stability. *Adv. Funct. Mater.* *17*, 3877–3884.
28. Zheng, J., Tan, G., Shan, P., Liu, T., Hu, J., Feng, Y., Yang, L., Zhang, M., Chen, Z., Lin, Y., et al. (2018). Understanding Thermodynamic and Kinetic Contributions in Expanding the Stability Window of Aqueous Electrolytes. *Chem* *4*, 2872–2882.
29. Yokoyama, Y., Fukutsuka, T., Miyazaki, K., and Abe, T. (2018). Origin of the Electrochemical Stability of Aqueous Concentrated Electrolyte Solutions. *J. Electrochem. Soc.* *165*, A3299–A3303.
30. Nakamoto, K., Sakamoto, R., Sawada, Y., Ito, M., and Okada, S. (2019). Over 2 V Aqueous Sodium-Ion Battery with Prussian Blue-Type Electrodes. *Small Methods* *3*, 1800220.
31. Nakamoto, K., Sakamoto, R., Ito, M., Kitajou, A., and Okada, S. (2017). Effect of Concentrated Electrolyte on Aqueous Sodium-ion Battery with Sodium Manganese Hexacyanoferrate Cathode. *Electrochemistry (Tokyo)* *85*, 179–185.
32. Weber, R., Genovese, M., Louli, A.J., Hames, S., Martin, C., Hill, I.G., and Dahn, J.R. (2019). Long cycle life and dendrite-free lithium morphology in anode-free lithium pouch cells enabled by a dual-salt liquid electrolyte. *Nat. Energy* *4*, 683–689.
33. Suo, L., Borodin, O., Sun, W., Fan, X., Yang, C., Wang, F., Gao, T., Ma, Z., Schroeder, M., von Cresce, A., et al. (2016). Advanced High-Voltage Aqueous Lithium-Ion Battery Enabled by “Water-in-Bisalt” Electrolyte. *Angew. Chem. Int. Ed. Engl.* *55*, 7136–7141.
34. Wessells, C., Ruffo, R., Huggins, R.A., and Cui, Y. (2010). Investigations of the Electrochemical Stability of Aqueous Electrolytes for Lithium Battery Applications. *Electrochem. Solid-State Lett.* *13*, A59.
35. Lee, M.H., Kim, S.J., Chang, D., Kim, J., Moon, S., Oh, K., Park, K.-Y., Seong, W.M., Park, H., Kwon, G., et al. (2019). Toward a low-cost high-voltage sodium aqueous rechargeable battery. *Mater. Today*.
36. Damjanovic, A., Dey, A., and Bockris, J. (1966). Kinetics of oxygen evolution and dissolution on platinum electrodes. *Electrochim. Acta* *11*, 791–814.
37. Aurbach, D., Gamolsky, K., Markovsky, B., Gofer, Y., Schmidt, M., and Heider, U. (2002). On the use of vinylene carbonate (VC) as an additive to electrolyte solutions for Li-ion batteries. *Electrochim. Acta* *47*, 1423–1439.